Available online at www.sciencedirect.com
SCIENCE DIRECT
Trans. Nonferrous Met. Soc. China 17(2007) 318−325
Transactions of Nonferrous Metals Society of China
www.csu.edu.cn/ysxb/

Corrosion behavior of aluminum alloy 2024-T3 by 8-hydroxy-quinoline and its derivative in 3.5% chloride solution

LI Song-mei(李松梅), ZHANG Hong-rui(张洪瑞), LIU Jian-hua(刘建华)

School of Materials Science and Engineering, Beijing University of Aeronautics and Astronautics, Beijing 100083, China

Received 25 May 2006; accepted 11 December 2006

Abstract: The corrosion behavior of aluminum alloy 2024-T3 was studied in 3.5% NaCl solution with two fluorescence quinoline compounds named 8-hydroxy-quinoline(8HQ) and 8-hydroxy-quinoline-5-sulfonic acid(HQS). The open circuit potential(OCP) test result indicates that both compounds change the alloy corrosion potential by adsorbing on the electrode surface. Polarization measurements show that 8HQ is a mixed type inhibitor by blocking the active sites of the metal surface, while HQS is a corrosion accelerator by activating the cathodic reaction. Changes of the impedance parameters in the electrochemical impedance spectroscopy(EIS) are related to the adsorption of 8HQ on the metal surface, which leads to the formation of a protective layer. The impedance diagram in the solution with HQS is similar to the one without additional organic compounds. The morphology and composition of the protective layer were studied by using SEM/EDS. The result confirms the function of the additions that the effect of 8HQ is due to the insoluble aluminum chelate, $Al(HQ)_3$, to prevent adsorption of chloride ion, while the effect of HQS is to break down the oxide film.

Key words: aluminum alloy; corrosion behavior; 8-hydroxy-quinoline; 8-hydroxy-quinoline-5-sulfonic acid; electrochemical impedance spectroscopy

1 Introduction

Aluminum alloys are widely used in the aeronautical industry and marine engineering due to their light mass and advantageous mechanical properties. However, these alloys have a low resistance against corrosion because of the presence of alloying elements which can locally break down the passive film and allow the attack of aggressive ions like chloride ions that can initiate pitting or crevice corrosion[1−4].

Generally, localized corrosion can be prevented and corrosion degree can be decreased by using corrosion inhibitors that can form a resistant oxide film on the metal surface to prevent aggressive ions. A number of corrosion inhibitors have been developed for this purpose. Chromates, which are passivating inhibitors, are recognized as being very efficient to inhibit the corrosion of aluminum and aluminum alloys[5−7]. The functions of this inhibitor are related to the interaction of chromate with the passive film and the formation of an insoluble chromium oxide Cr_2O_3 that can repair the defects of the passive film[8−9]. But the strong oxidizing properties of Cr(Ⅵ) and its carcinogenesis make chromates harmful to the environment, therefore it is necessary to obtain a new corrosion inhibitor for aluminum and its alloys to replace chromates. Cerium has been proved to be a viable replacement for chromates[10−11], which acts as a cathodic inhibitor by forming a cerium rich layer to inhibit the cathodic reaction[12]. Phosphate is another inorganic corrosion inhibitor replacement of chromates [13]. It is usually used in conversion coating baths to form insoluble phosphate-aluminum layer and reduce significantly the hydration rate of Al oxide[14].

Some organic compounds have been also used as corrosion inhibitors which often contain nitrogen, oxygen, sulfur and ring system. Benzotriazole(BTA) is a well known inhibitor[15]. It absorbs on the metal surface

Foundation item: Project(50571003) supported by the National Natural Science Foundation of China
Corresponding author: LI Song-mei; Tel/Fax: +86-10-82317103; E-mail: songmei_li@buaa.edu.cn

by chemical bond to act as an anodic inhibitor preventing chloride or other aggressive ions interacting with the metal. Other organic amines containing nitrogen are also considered aluminum corrosion inhibitors in neutral and acidic medium[16].

In our previous study[17], 8-hydroxy-quinoline and its derivative 8-hydroxy-quinoline-5-sulfonic acid were used as corrosion sensors for aluminum alloys, which were added into acrylic or epoxy coatings. They were sensitive to the corrosion product Al^{3+} or pH value during corrosion process by changing their fluorescence character. Some researchers have found that 8-hydroxy-quinoline is effective for preventing pitting corrosion of aluminum alloys by forming an insoluble chelate complex layer. GARRIGUES et al[18] investigated the corrosion inhibition of pure aluminum by 8-hydroxy-quinoline in neutral and acidic chloride solutions. They concluded that 8-hydroxy-quinoline acts on the passive alumina layer to prevent the adsorption of chloride ions and the destruction of aluminum oxide film.

The present study was designed to investigate corrosion behavior of AA 2024-T3 in 3.5% sodium chloride solution by 8-hydroxy-quinoline and 8-hydroxy-quinoline-5-sulfonic acid. Polarization measurements were employed to discuss the effect of 8HQ and HQS. Electrochemical impendence spectroscopy(EIS) was used to investigate the mechanisms, and surface analysis (SEM/EDS) were used to observe the microstructure.

2 Experimental

2.1 Material

Corrosion inhibition investigations were performed on AA2024-T3 (nominal composition: 4.5% Cu, 1.5% Mg, 0.6% Mn, 0.2% Fe, 0.06% Si, 0.08% Zn, 0.03% Ti, balance Al), supplied in the form of a 1 mm thick plate. Exposed specimens were prepared by cutting coupons of 50 mm × 30 mm from the plates. Before testing, specimens were mechanically polished with 1200 grit SiC paper, and then with 1.5 μm diamond paste. They were finally rinsed with distilled water. 8-hydroxy-quinoline(8HQ) and 8-hydroxy-quinoline-5-sulfonic acid(HQS) were analytical grade reagent (purity ＞99%) and the compound structure was shown in Fig.1. The concentration of 8-hydroxy-quinoline was 3.8×10^{-3} mol/L, which is near the solubility limit. For comparison the concentration of 8-hydroxy- quinoline-5-sulfonic was 3.8×10^{-3} mol/L too. The corrosion medium was a 3.5% solution of NaCl (reagent grade).

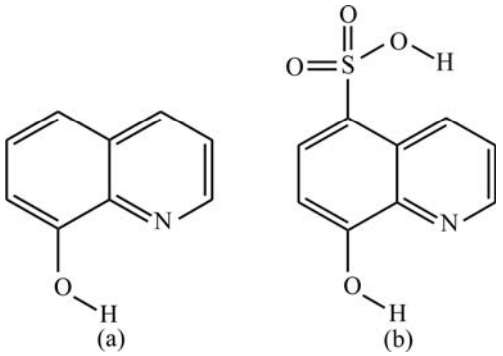

Fig.1 Molecule structures of 8HQ (a) and HQS (b)

2.2 Electrochemical measurements

Electrochemical measurements were carried out using an EG&G Princeton Applied Research Parc Model 2273. A three-electrode configuration was employed with AA2024-T3 acting as working electrode, a platinum panel as the auxiliary electrode and a saturated calomel electrode(SCE) as reference. The area of working electrode was 10 mm×10 mm, and the same disposing process as above was taken before testing. The OCP was measured for 10 h. The potentiodynamic polarization measurement was performed from −0.6 V (vs OCP) to 0.25 V (vs OCP). EIS measurements were carried out by applying to the cell a 10 mV sine wave with frequencies in the range of 100 kHz−5 mHz.

2.3 Surface analysis

The surface analysis of AA2024-T3 was investigated by means of SEM (JEOL SEM5800) equipped with an EDS probe (accelerator voltage was 20 keV) after 4 d of immersion in the corrosive medium with or without fluorescence compounds.

3 Results and discussion

3.1 Electrochemical behavior of AA2024-T3 in 3.5%NaCl solution containing 8HQ and HQS

The variations of the open circuit potential of AA2024-T3 with time in a 3.5% neutral chloride solution in presence of 8HQ or HQS at room temperature are shown in Fig.2. Under the experimental condition, two features can be distinguished from the obtained curves. Firstly, for two kinds of solution, the open circuit potential shifts in the anodic direction and then reaches steady-state values. The corrosion potential in the solution with 8HQ moves from −0.86 V to −0.83 V, while in the solution with HQS the corrosion potential strongly shifts to more positive value, from −0.75 V to −0.69 V. Secondly, the whole evolution of the OCP

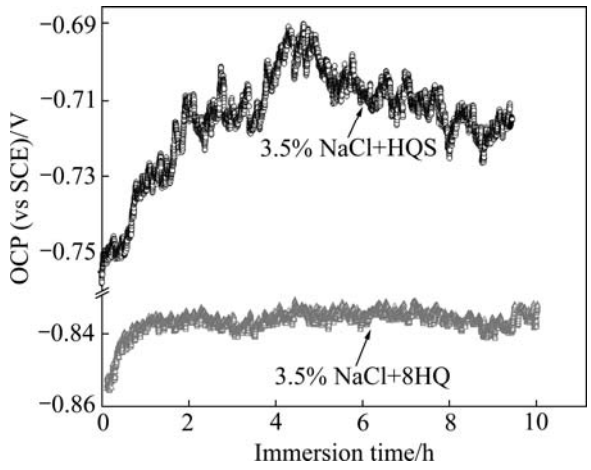

Fig.2 Open circuit potential—time curve in NaCl solution with 8HQ and HQS

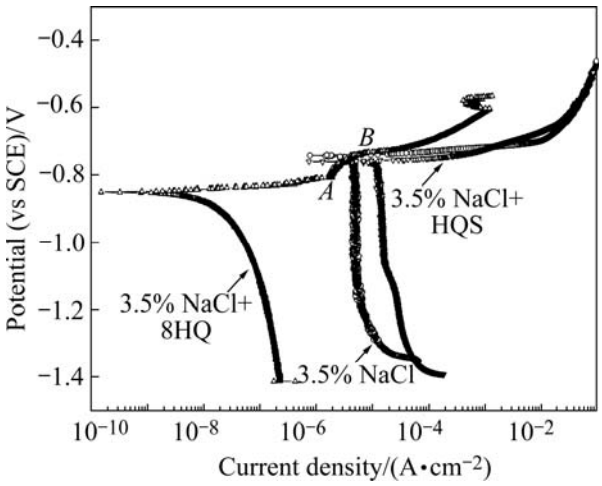

Fig.3 Polarization curve in NaCl solution with or without fluorescence compounds

potential with immersion time is different in the presence of two fluorescence compounds. The OCP is very steady after the first hour in the solution with 8HQ, but it does not keep stable until 8 h later in the solution with HQS.

Many researchers have discussed the open circuit potential change of the aluminum alloys in the chloride solution[19−20]. In NaCl solution, the corrosion potential shifts to cathodic value after a short period of immersion time due to the adsorption of chloride ions. With increasing immersion time, the corrosion potential goes towards a more positive value and keeps constant since the hydration of the oxide film and the formation of pre-layer $Al(OH)_3$. In the presence of 8HQ, the adsorption of chloride is slowed down by the competitive absorption of 8HQ and the corrosion potential slowly shifts to anodic value untill the absorption of 8HQ becomes stable. It can be explained by the formation of 8HQ-Al layer that prevents the dissolution of the pre-formed oxide layer on the aluminum electrode.

In the presence of HQS, the evolution of the OCP potential is due to the absorption of HQS. Although HQS has the similar structure to the 8HQ, the property is very different with the latter because of the presence of —HSO_3 group that has aggressive ability like the chloride ions. The absorption of —HSO_3 inhibits the formation of oxide film and accelerates the dissolution of the alloy matrix. The process results in the corrosion potential moving in anodic direction.

Fig.3 presents the potentiodynamic polarization curves in 3.5% NaCl solution with or without fluorescence compounds for AA2024-T3. In NaCl solution，there is a strong increase above the open circuit potential in current density that corresponds to the breakdown potential −0.72 V[21]. In the NaCl solution with HQS, the anodic polarization curve is identical with the blank one and the breakdown potential is not modified by the HQS. This means that HQS does not affect the anodic behavior. On the other hand, the cathodic current densities are higher than those in the NaCl solution, so the oxygen reaction is accelerated.

In the NaCl solution with 8HQ, the cathodic and anodic current densities are both much lower than those in NaCl solution, which indicates that oxygen reduction and alloy substrate dissolution process are limited by 8HQ that acts as a mixed type inhibitor, inhibiting the corrosion of aluminum alloy by blocking the active sites of the metal surface. In addition, a current plateau is observed in the anodic direction (*AB*). GARRIGUES et al[18] also found the same phenomena in the polarization curve of pure aluminum with 8HQ. LI and DRAZIC et al[22] considered it related to the anodic desorption of the absorbed compounds. EIS measurement was employed to studying the behaviors of absorption and desorption of 8HQ below.

3.2 EIS measurement in 3.5% NaCl solution containing 8HQ

Electrochemical impedance spectroscopy(EIS) has already been successfully used in corrosion and protection fields since it can provide information on the corrosion and protection mechanisms, especially for an adsorbed film[23]. Figs.4(a) and (b) show the electrochemical impedance diagrams (in Nyquist format (a) and in Bode phase vs f format(b)) at the corrosion potential after different immersion time when 8HQ was added to the sodium chloride solution and Figs.5(a) and (b) show the electrochemical impedance diagrams in the inhibitor-free NaCl solution.

As shown in Fig.4(a), the great increase in the

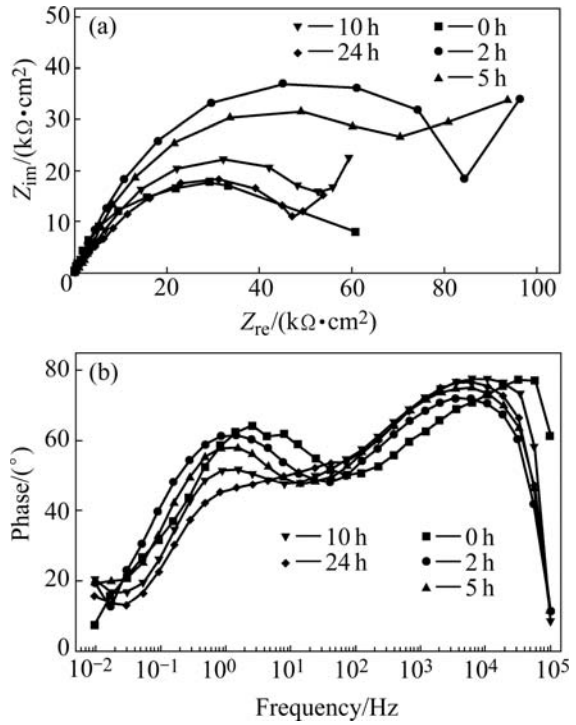

Fig.4 EIS diagrams obtained at open circuit potential after different immersion time in NaCl solution with 8HQ: (a) Nyquist format; (b) Bode diagrams

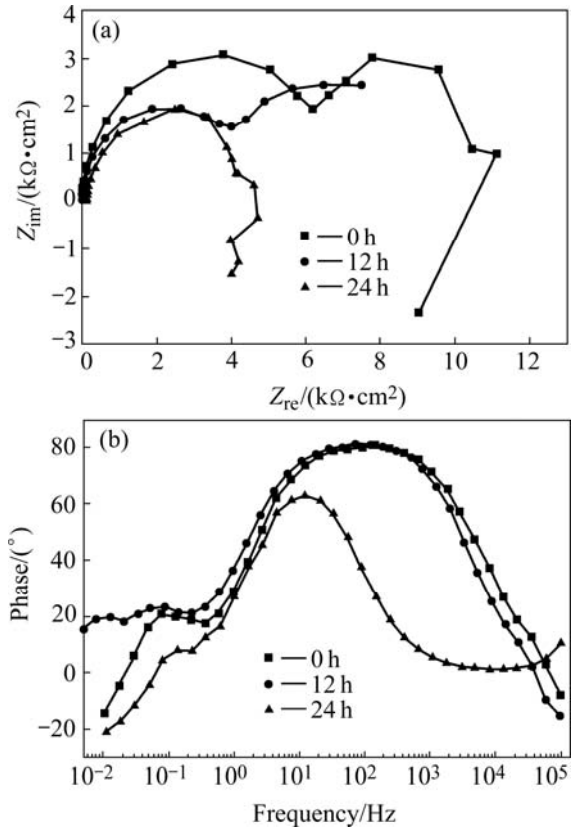

Fig.5 EIS diagrams obtained at open circuit potential after different immersion time in inhibitor-free NaCl solution: (a) Nyquist format; (b) Bode diagrams

diameter of Nyquist semi-circles in the first 2 h suggests that the presence of 8HQ changes the corrosion kinetics on the electrode surface. The Bode diagrams that were plotted using the same experimental data in the Nyquist format show a new phase angle shift at high frequency range compared with the one obtained in the inhibitor-free solution. The new phase shift means that the formation of inhibitor film changes the electrode interfacial structure and results in an extra time constant. Two peaks in the Bode plots indicate that there are two major electrochemical kinetic processes on the electrode surface: The high frequency part is due to the adsorption of the 8HQ molecule and the formation of the inhibitor film; the second time constant at medium frequency is due to the electrochemical corrosion process[24]. And then, the diameter of Nyquist semi-circles becomes smaller. It can be explained by the damage of the inhibitor film in the chloride solution.

The impedance characteristics of this electrode surface could be simulated by an electrical circuit as Fig.6. R_{sol} is the resistance of the solution; R_{ing} is the resistance of the inhibitor layer; C_{ing} is the capacitance of the inhibitor film; C_{al} is the capacitance and R_{al} is the resistance of the oxide film; C_d is the double layer capacitance; R_p is the electrochemical charge transfer resistance.

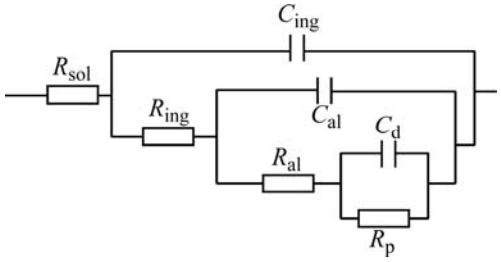

Fig.6 Equivalent circuit model for fitting experimental results with 8HQ

Fig.7 depicts the evolution of the double layer capacitance C_d and the polarization resistance R_p during immersion of AA2024-T3 in the solution containing 8HQ. In the first 2 h, the polarization resistance R_p greatly increases and the double layer capacitance C_d decreases due to the formation of the inhibitor layer that limits the corrosion process. A high polarization resistance and a low double layer capacitance reveal good inhibition of 8HQ. This result identifies the OCP experiment. The polarization resistance R_p decreases and the double layer capacitance C_d increases after 2 h. A possible explanation for this change may be localized breakdown of the inhibitor layer.

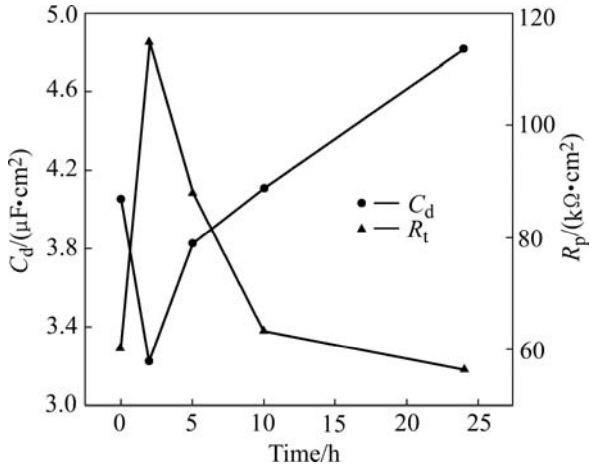

Fig.7 Evolution of double layer capacitance and polarization resistance during immersion of AA2024-T3 in electrolytes with 8HQ

As discussed in section 3.1, a current plateau is observed in the anodic polarization curve in the NaCl solution containing 8HQ, which stands for the desorption process of the 8HQ molecule. In Fig.8, the impedance data recorded in 3.5% NaCl solution with 8HQ at open circuit potential(OCP), OCP+40 mV (point *A*) and OCP+80 mV (point *B*) for AA2024-T3 electrode are presented. At OCP, the Nyquist plots are purely capacitive and the polarization resistance is very high, about 60.15 kΩ/cm^2. The adsorption layer with 8HQ represents a good corrosion inhibition action at this potential. At OCP+40 mV, just little lower than the desorption potential (point *A*), an inductive behavior is observed, which indicates that the layer with 8HQ is in unstable estate and desorption process will occur. At OCP+80 mV (point *B*), although the potential moves 40 mV in anodic direction, the polarization resistance greatly drops. The inhibitor layer has desorbed completely at this potential and the electrode surface has changed like one without inhibitor.

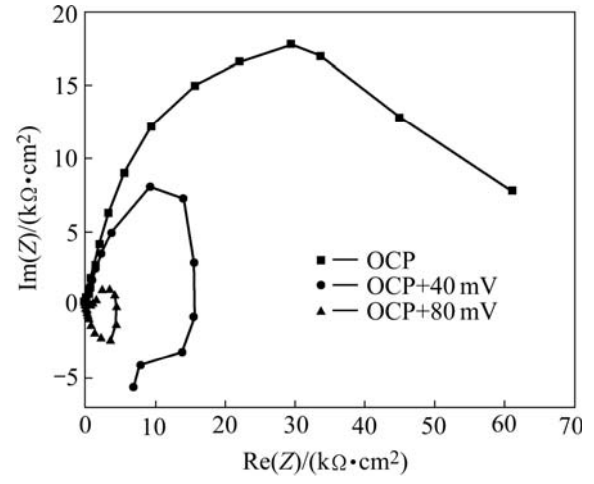

Fig.8 Electrochemical impedance diagrams obtained at open circuit potential (a), OCP+40 mV (b) and OCP+80 mV (c) in solution containing 8HQ

3.3 EIS measurement in 3.5% NaCl solution containing HQS

Fig.9 shows the electrochemical impedance diagrams at the corrosion potential after different immersion time in 3.5% NaCl solution containing HQS. The diagrams are similar to ones in 3.5% NaCl solution, from which it can be considered that the electrode surface and reaction mechanism are not changed by the addition of HQS. The polarization resistance decreases along with immersion time due to the breakdown of the oxide film. In this situation, HQS acts as an aggressive compound like chlorine ions. The reaction process can be explained by 4 steps below:

1) The adsorption process of HQS: the structure of HQS has S atom, so it is easier for HQS to adsorb on the aluminum surface than 8HQ;

2) The decomposition process of HQS: —HSO_3 appears due to the decomposition of HQS;

3) The breakdown of oxide film due to —HSO_3 and Cl^-;

4) The dissolution of the matrix.

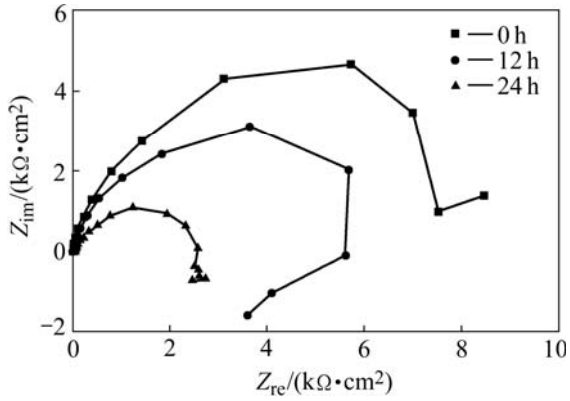

Fig.9 Electrochemical impedance diagrams obtained at open circuit potential after different immersion time in NaCl solution with HQS

3.4 Microscopic observations

The polished AA2024-T3 specimens were immersed in 3.5% NaCl solution with or without fluorescence compounds to estimate the evolution of the alloy surface. Optical micrographs of the substrate after 4 d of testing are presented in Fig.10. The sample in chloride solution (Fig.10(a)) only shows obvious changes of the surface due to localized corrosion processes. Dark areas formed around the pits indicate redeposition of

copper dissolved from the intermetallic particles[25]. It is assumed that the preferential dissolution of the matrix surrounding the coarse intermetallic particles is caused by the existence of a galvanic couple between, on one hand the copper depleted dispersoid-free zone and the rest of the matrix, and on the other hand the copper depleted dispersoid-free zone and the Al_2CuMg chemical combination (*S* phase)[26]. In addition, *S* phase particles are subject to bulk dealloying through preferential dissolution of magnesium, but the release of copper is also plausible since the particles are often surrounded by copper deposits. It has been identified by BUCHHEIT et al [27] that these deposits are mostly copper deposits originating from the S-phase particles.

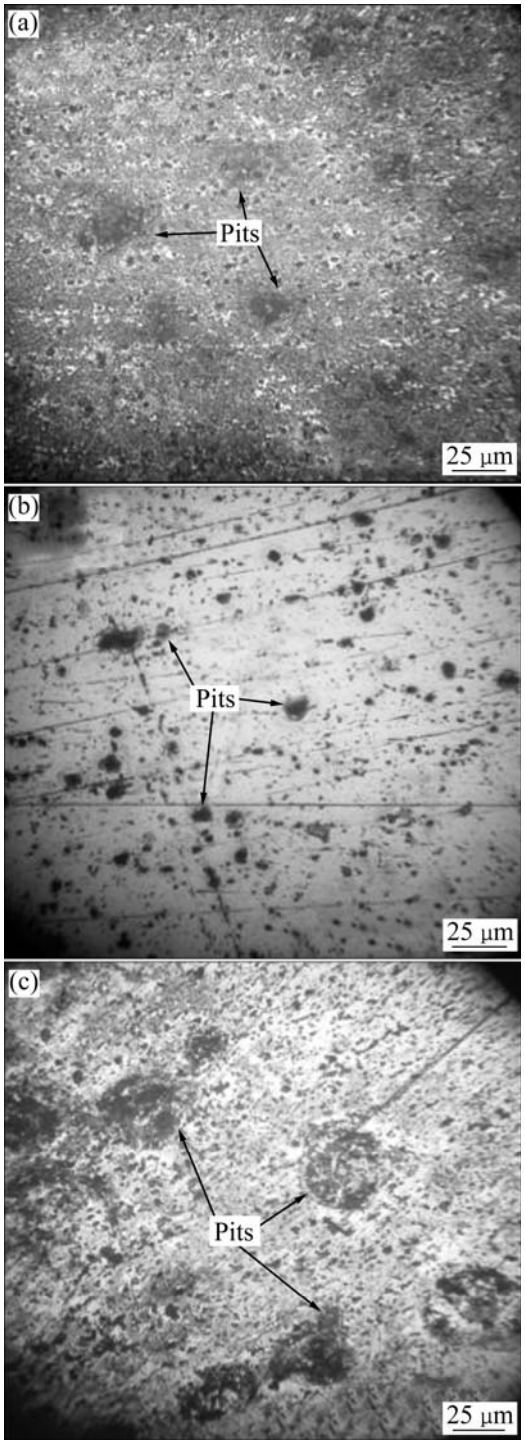

Fig.10 Photographs of aluminum surface after testing for 4 d: (a) Without fluorescence compounds; (b) In presence of 8HQ; (c) In presence of HQS

The sample immersed in the solution with 8HQ shows only the first signs of corrosion activity in zones of the intermetallic particles (Fig.10(b)), while obvious corrosion sites can be seen in the sample surface immersed in the solution with HQS (Fig.10(c)).

Finally, Fig.11 shows scanning electronic microscopy (SEM) images of the AA2024-T3 sample surfaces. The image of the surface exposed to the solution without 8HQ and HQS (Fig.11(a)) shows a heterogeneous layer of products and cracked surface appears. EDS analysis further identifies characteristic corrosion product elements (mainly Cu, Fe, Mn, Al, O and Cl) on this layer. It is assumed that the local corrosion occurs at the position of *S*-phase and the heterogeneous layer is around the (Cu, Fe, Mn)Al_6 intermetallic particles[28].

The SEM image obtained in the presence of 8HQ (Fig.11(b)) shows that the addition of this compound markedly modifies the properties of the layer at the electrode surface where no sign of dissolution of the surrounding bulk matrix is observed and smooth patchy deposits are also observed on some *S*-phase particle surfaces. It is clear that 8HQ strongly inhibits the dealloying of *S*-phase particles. However, analyses of the specimen surface by EDS reveal that the presence of a small quantity of N and C is only on the deposit particles. These particles seem to be attacked, and the grain structure is visible in the crack of the deposit. EIS analysis indicates that the inhibitor promotes the formation of a much homogeneous layer to cover the active sites and remains incorporated in its structure. Such a corrosion product film is formed by the interaction of aluminum with 8HQ. The main process of inhibition in the 8HQ case seems to be the adsorption of the 8HQ on the aluminum anode, which slows down the corrosion rate and prevents the adsorption of chloride ion and thus the destruction of the aluminum oxide film. It is possible that an insoluble chelate of aluminum, $Al(HQ)_3$, may be formed and compete with the formation of the insulating aluminum hydroxide[29].

The SEM image obtained in the presence of HQS (Fig.11(c)) shows that the oxide film has been seriously destroyed and the characteristic of intergranular corrosion can be observed. Element S is detected by EDS analysis. This result identifies the EIS measurement that

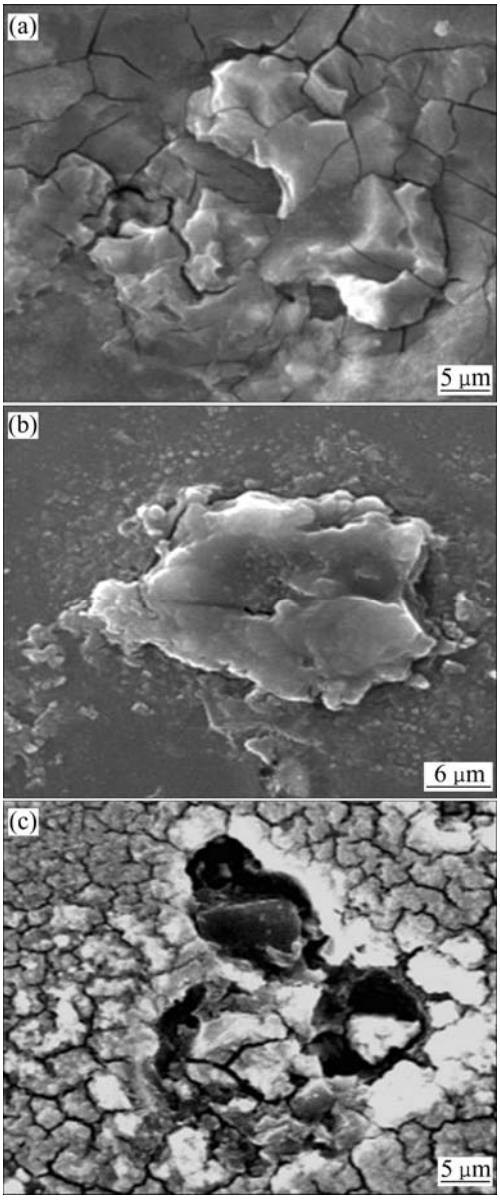

Fig.11 SEM micrographs of aluminum alloy surface: (a) Without fluorescence compounds; (b) In presence of 8HQ; (c) In presence of HQS

HQS acts as aggressive compound like the chloride ion.

4 Conclusions

1) 8HQ is a mixed inhibitor for AA2024-T3, which decreases the rate of both anodic and cathodic reaction by forming a protective film on the alloy surface. While HQS is a corrosion accelerator, mainly activating the cathodic process, although it has similar structure to the 8HQ.

2) EIS measurement expresses the significant adsorption of 8HQ on the aluminum surface, which prevents oxide film from chloride ion. The impedance diagrams obtained in the solution with HQS is so similar to one without it, where the effect of HQS is like chloride ion.

3) The microscopic observation results, the electrochemical measurements and EIS results show that the inhibitive mechanism of 8HQ is related to the adsorption layer, while the corrosion accelerative effect is due to $—HSO_3$.

References

[1] YU S Y, O'GRADY W E, RAMAKER D E, NATISHAN P M. Chloride ingress into aluminum prior to pitting corrosion: An investigation by XANES and XPS [J]. J Electrochem Soc, 2000, 147: 2952−2958.

[2] SZKLARSKA-SMIALOWSKA Z. Pitting corrosion of aluminum [J]. Corr Sci, 1999, 41: 1743−1767.

[3] LEE E J, PYUN S I. The effect of oxide chemistry on the passivity of aluminum surfaces [J]. Corr Sci, 1995, 37: 157−168.

[4] FRANKEL G S. Pitting corrosion of metals: A review of the critical factors [J]. J Electrochem Soc, 1998, 145: 2186−2198.

[5] OLIVERA-BRETT A M, BRETT C M A, SILVA L A. An impedance study of the adsorption of nucleic acid bases at glassy carbon electrodes [J]. Bioelectrochemistry, 2002, 56: 33−35.

[6] AKIYAMA E, MARKWORTH A A J, MCCOY A J K, FRANKEL C G S, XIA A L B, MCCREERYB R L. Storage and release of soluble hexavalent chromium from chromate conversion coatings on Al alloys: Kinetics of release [J]. J Electrochem Soc, 2003, 150: 83−91.

[7] WAINRIGHT J S, MURPHY Q J, ANTONIO M R. The oxidation state and coordination environment of chromium in a sealed anodic aluminum oxide film by X-ray absorption spectroscopy [J]. Corr Sci, 1992, 33: 281−293.

[8] MCCAFFERTY E. A surface charge model of corrosion pit initiation and of protection by surface alloying [J]. J Electrochem Soc, 1999, 146: 2863−2869.

[9] KOLICS A, BESING S, WIECKOWSKI A. Interaction of chromate ions with surface intermetallics on aluminum alloy 2024-T3 in NaCl solutions [J]. J Electrochem Soc, 2001, 148: 322−331.

[10] KENDIG M, JEANJAQUET S, ADDISON R, WALDROP J. Role of hexavalent chromium in the inhibition of corrosion of aluminum alloys [J]. Surf Coat Tech, 2001, 140: 58−66.

[11] ALDYKEWICZ A J, ISAACS H S, DAVENPORT A J. The investigation of cerium as a cathodic inhibitor for aluminum-copper alloys [J]. J Electrochem Soc, 1995, 142: 3342−3350.

[12] WIERZCHO T, ULBIN-POKOSKA I, SIKORSKIi K. Corrosion resistance of chromium nitride and oxynitride layers produced under glow discharge conditions [J]. Surf Coat Tech, 1995, 130: 274−279.

[13] SUSAC D, SU X, LI R Y, WONG K C, WONG P C, MITCHELL K A R, CHAMPANERIA R. Microstructural effects on the initiation of zinc phosphate coatings on 2024-T3 aluminum alloy [J]. Appl Surf Sci, 2004, 239: 45−59.

[14] KOLICS A, WASZCZUK A P, GÁNCS A L, NÉMETH B Z, WIECKOWSKIA A. Enhancement and inhibition of phosphate deposition on aluminum [J]. Electrochem Solid State Lett, 2000, 3: 369−372.

[15] GOMMA G K. Corrosion inhibition of steel by benzotriazole in sulphuric acid [J]. Mat Chem Phys, 1998, 55: 235−240.

[16] SANAD S H, ABBAS H, ISMSIL A A, EI-SOBLI K M. Benzotriazole as a corrosion inhibitor for brass [J]. Surf Tech, 1985, 25: 39−48.

[17] LI S M, ZHANG H R, LIU J H. Preparation and performance of fluorescence sensing coating for monitoring corrosion of Al alloy 2024 [J]. Trans Nonferrous Met Soc, 2006, 16(s1): 159−164.

[18] GARRIGUES L, PEBERE N, DABOST F. An investigation of the corrosion inhibition of pure aluminum in neutral and acidic chloride

solutions [J]. Electrochimica Acta, 1996, 41: 1209−1215.

[19] KOLICS A, BESING A A S, BARADLAI A P, HAASCH A R, WIECKOWSKIA A. Effect of pH on thickness and ion content of the oxide film on aluminum in NaCl media [J]. J Electrochem Soc, 2001, 148: B251−259.

[20] CECCHETTO L, AMBAT R, DAVENPORT A J, DELABOUGLISE D, PETIT J P, NEEL Q. Emeraldine base as corrosion protective layer on aluminium alloy AA5182, effect of the surface microstructure [J]. Corr Sci, 2007, 49: 818−829.

[21] GUILLAUMIN V, MANKOWSKI G. Localized corrosion of 2024 T351 aluminum alloy in chloride media [J]. Corr Sci, 1999, 41: 421−438.

[22] LI M, DRAZIC D M. Adsorption and corrosion inhibitive properties of some organic molecules on iron electrode in sulfuric acid [J]. Corr Sci, 2002, 44: 1669−1680.

[23] TAN Y J, BAILEY S, KINSELLA B. An investigation of the formation and destruction of corrosion inhibitor films using electrochemical impedance spectroscopy (EIS) [J]. Corr Sci, 1996, 38: 1545−1561.

[24] THOMPSOM I, CAMPBELL D. Interpreting Nyquist responses from defective coatings on steel substrates [J]. Corr Sci, 1994, 36: 187−198.

[25] ZHELUDKEVICH M L, YASAKAU K A, POZNYAK S K, FERREIRA M G S. Triazole and thiazole derivatives as corrosion inhibitors for AA2024 aluminum alloy [J]. Corr Sci, 2005, 47: 3368−3383.

[26] GUILLAUMIN V, MANKOWSKI G. Localized corrosion of 2024 T351 aluminium alloy in chloride media [J]. Corr Sci, 1999, 41: 421−438.

[27] BUCHHEIT R G, MARTINEZ M A, ONTES L P. Evidence for Cu ion formation by dissolution and dealloying the Al_2CuMg intermetallic compound in rotating ring-disk collection experiments [J]. J Electrochem Soc, 2000, 147: 119−124.

[28] WALDROP J R, KENDIG M W. J Nucleation of chromate conversion coating on aluminum 2024-T3 investigated by atomic force microscopy [J]. J Electrochem Soc, 1998, 145: 11−13.

[29] SABINE SZUNERITS, WALT D R. Aluminum surface corrosion and the mechanism of inhibitors using pH and metal ion selective imaging fiber bundles [J]. Anal Chem, 2002, 74: 886−894.

(Edited by YANG Hua)